Journal of NeuroEngineering and Rehabilitation

RESEARCH

Open Access

Enhanced gait tracking measures for individuals with stroke using leg-worn inertial sensors

Francesco Lanotte[1,2†], Shusuke Okita[1,2†], Megan K. O'Brien[1,2] and Arun Jayaraman[1,2,3*]

Abstract

Background Clinical gait analysis plays a pivotal role in diagnosing and treating walking impairments. Inertial measurement units (IMUs) offer a low-cost, portable, and practical alternative to traditional gait analysis equipment, making these techniques more accessible beyond specialized clinics. Previous work and algorithms developed for specific clinical populations, like in individuals with Parkinson's disease, often do not translate effectively to other groups, such as stroke survivors, who exhibit significant variability in their gait patterns. The Salarian gait segmentation algorithm (SGSA) has demonstrated the potential to detect gait events and subsequently estimate clinical measures of gait speed, stride time, and other temporal parameters using two leg-worn IMUs in individuals with Parkinson's disease. However, the distinct gait impairments in stroke survivors, including hemiparesis, spasticity, and muscle weakness, can interfere with SGSA performance. Thus, the objective of this study was to develop and test an enhanced gait segmentation algorithm (EGSA) to capture temporal gait parameters in individuals with stroke.

Methods Forty-one individuals with stroke were recruited from two acute rehabilitation settings and completed brief walking bouts with two leg-worn IMUs. We compared foot-off (FO), foot contact (FC), and temporal gait parameters computed from the SGSA and EGSA against ground truth measurements from an instrumented mat.

Results The EGSA demonstrated greater accuracy than the SGSA when detecting gait events within one second, for both FO (96% vs. 90%) and FC (94% vs. 91%). The EGSA also demonstrated lower error than the SGSA when detecting paretic FC, and FO events in slow, asymmetrical, and non-paretic footfalls. Temporal gait parameters from the EGSA had high reliability (ICC > 0.90) for stride time, step time, stance time, and double support time across gait speeds and levels of asymmetry.

Conclusion This approach has the potential to enhance the accuracy and validity of IMU-based gait analysis in individuals with stroke, thereby enhancing clinicians' ability to monitor and intervene for gait impairments in a rehabilitation setting and beyond.

†Francesco Lanotte and Shusuke Okita equally contributed to the work and should be considered co-first authors.

*Correspondence:
Arun Jayaraman
a-jayaraman@northwestern.edu

[1]Max Nader Lab for Rehabilitation Technologies and Outcomes Research, Shirley Ryan AbilityLab, 355 E Erie St, Chicago, IL 60611, USA
[2]Department of Physical Medicine and Rehabilitation, Northwestern University, 710 N Lake Shore Dr, Chicago, IL 60611, USA
[3]Department of Physical Therapy and Human Movement Science, Northwestern University, 710 N Lake Shore Dr, Chicago, IL, USA60611

Introduction

Inertial measurement units (IMUs) can obtain high-resolution gait parameters in diverse environments with minimal obtrusiveness. With judicious signal processing algorithms, these wearable sensors offer precision comparable to that of cumbersome and expensive motion analysis equipment [1, 2]. These sensors can be leveraged in clinical gait analysis and rehabilitation medicine to detect abnormal gait patterns and biomarkers of impairment [3, 4]. Integrating these devices into therapy planning would enable clinicians to monitor changes in gait impairment, supplementing traditional functional outcomes of gait speed, endurance, and balance [5–7].

Effective, reliable algorithms are needed to extract meaningful gait measures from raw IMU signals. Although numerous studies have demonstrated the validity and reliability of IMU-based gait parameters *within* various populations and clinical settings (i.e., by detecting and segmenting key parts of the gait cycle) [8–10], these measures have remained largely untested *across* individuals with different gait impairments. Examining an algorithm's validity in different subgroups of patients is critical to define and understand its potential use cases. If an algorithm performs insufficiently, it may not be practical for clinical use. Further development of the population-specific or even person-specific algorithms may be warranted [11]. This approach can maximize the validity of gait parameters for effective implementation, and it can guide clinicians and researchers to interpret measures generated by different algorithms [12, 13].

Stroke is one such condition that may challenge the performance and usability of IMU systems for clinical gait analysis. Distinct motor impairments after stroke (including hemiparesis, spasticity, muscle weakness, limited balance and coordination) result in asymmetric, slow, and irregular gait patterns, as well as limited knee flexion and ankle dorsiflexion [14, 15]. We previously examined IMU-derived gait parameters from a commercial IMU system in a chronic stroke population, finding greater error during slower walking and more asymmetric gait [16]. Such errors would limit the usability of an IMU system in Inpatient Rehabilitation Facilities (IRFs), where patients experience more extensive and fluctuating gait impairments compared to chronic populations [17]. Notably, there have been a limited number of algorithms developed or validated specifically in stroke populations [4]. In one example, Yang et al. (2013) applied IMUs on the lower legs in 13 individuals with post-stroke hemiparetic gait [18]. They utilized acceleration and angular velocity signals to compute walking speed and to segment different parts of the gait cycle, respectively. While their approach generally performed well when estimating walking speed, there was no comparative ground truth measurement to validate the gait segmentation performance, and the authors acknowledged that their algorithm failed for subjects with abnormal shank angular velocities. Thus, more robust methods are needed to address the range of gait patterns seen in broader stroke populations. Specialized gait segmentation algorithms may be necessary to adapt to and accurately interpret these varied stroke-related gait abnormalities [19].

One such gait segmentation algorithm, presented by Salarian and colleagues, was designed to detect mid-swing, foot-off (FO), and foot contact (FC) gait events based on characteristic angular velocity patterns during walking, as measured by two IMUs on the lower legs [20]. Originally designed using IMU data from people with Parkinson's disease, which typically manifests in gait as a global impairment, marked by bradykinesia and shuffling [21], this algorithm has been applied to various healthy and clinical populations for gait monitoring [22], deriving spatial gait parameters [23], and computing features for predictive models [24]. However, the sole reliance of Salarian's gait segmentation algorithm (SGSA) on angular velocity could lead to misdetections or failures when applied to populations with different gait abnormalities, such as stroke survivors.

Unlike Parkinson's disease, stroke-related gait impairments often include hemiparesis, spasticity, and muscle weakness, leading to asymmetric, slow, and irregular gait patterns [25]. Specifically, hemiparesis leads to uneven weight distribution and altered swing phases between the paretic and non-paretic legs [26, 27], causing irregular patterns that gyroscopes may not consistently detect [28]. Spasticity and muscle weakness contribute to unpredictable and hesitant movements, resulting in irregular angular velocity signals that can obscure the precise identification of gait events [29]. Additionally, slower walking speeds amplify the variability in limb movements, making it more challenging for gyroscope-based algorithms to maintain accuracy in event detection. These complexities can hinder an algorithm's ability to reliably segment the gait cycle by making it difficult to differentiate between genuine gait events and other motions introduced by post-stroke impairments. To address these challenges, we developed and tested an enhanced gait segmentation algorithm (EGSA), an adaptation of the SGSA specifically for individuals with subacute stroke.

The objectives of this study were twofold: (i) to benchmark the gait events and temporal gait parameters derived from the SGSA and the EGSA against a commonly used reference system, the GAITRite instrumented mat, and (ii) to compare the performance of the EGSA against the SGSA across different levels of speed and symmetry in subacute stroke. We hypothesized that the EGSA would be more sensitive than the SGSA when identifying gait events for individuals with stroke exhibiting slow and asymmetric gait.

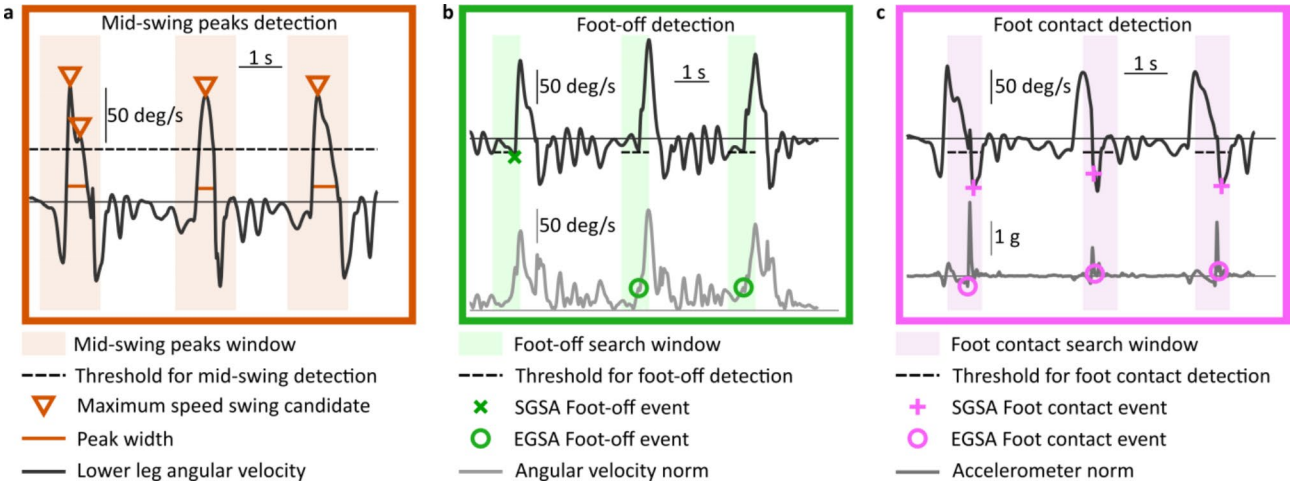

Fig. 1 The three main steps of both the SGSA and EGSA to detect the (**a**) mid-swing, (**b**) foot-off, and (**c**) foot contact events. The solid horizontal line demarks the 0 for all the signals

Methods

Gait segmentation algorithms

Both the SGSA and EGSA leverage a continuous angular velocity signal from the lower leg IMUs (gyroscope horizontal axis; ω_h, aligned with the mediolateral axis of the leg) [20], chosen for its applicability across healthy and pathological gait [22, 30]. In this context, positive values of ω_h indicate lower leg extension, while negative values signify lower leg flexion. Both algorithms segment key phases of the gait cycle by detecting mid-swing, foot-off (FO), and foot contact (FC) (Fig. 1). The SGSA utilizes a threshold-based approach to detect the mid-swing event by detecting positive peaks of ω_h and labeling the local minima before and after these peaks as FO and FC, respectively (Fig. 1). The EGSA retains similar methods for identifying mid-swing but enhances FO detection by integrating the norm of the angular velocity signals to capture the residual propulsive movement of the lower leg. For FC detection, the EGSA supplements the FC events from SGSA with those derived from the acceleration signal from the lower leg IMUs (accelerometer norm), to capture the leg's deceleration for precise foot placement. Additionally, it uses dynamic time warping (DTW) to identify which FC events produce a segmentation with minimum distance from a template for normal gait patterns. Additional details about the SGSA and EGSA are provided in the Supplementary Materials.

Participants

Forty-one participants with stroke were recruited from inpatient care units at the Shirley Ryan AbilityLab (Chicago, IL), and Ascension Alexian Brothers (Elk Grove Village, IL). Inclusion criteria were: age 18 or older; individuals diagnosed with stroke admitted to either hospital; able and willing to give written consent and comply with study procedure. Exclusion criteria were: diagnosis of neurodegenerative pathologies; individuals who are pregnant or nursing; individuals with skin allergies, irritation, or open wounds; and individuals with a powered, implanted cardiac device. Demographics and clinical characteristics of these participants are provided in Table 1. Additionally, 51 healthy individuals (17 F/22 M, age 62.3 ± 14.3) with no known neurological or musculoskeletal conditions were recruited as comparative controls, and their data was used for DTW template in the EGSA. The study was approved by the Institutional Review Board of Northwestern University (Chicago, IL; STU00205532) under federal regulations, university policies, and ethical standards regarding research on human subjects.

Table 1 Participant demographics. Mean and standard deviation (SD) are presented. Two participants were not included in the table, as they were withdrawn due to medical complications after consenting

	***n* = 39**
Age (years)	62.3 ± 14.3
Sex (Male/Female)	22/17
Height	172.0 ± 10 cm
Weight	91.1 ± 27.0 kg
Days since stroke	17.0 ± 11.9 days
Stroke type (Ischemic/Hemorrhagic)	30/9
Paretic side (Left/Right)	16/23

Experimental protocol

Participants with stroke completed up to seven study visits: within one week of IRF admission, within one week prior to discharge, and 1-, 3-, 6-, 9-, and 12-months post-stroke, with each session lasting up to 2 h. At each visit, participants were asked to complete a series of standardized clinical assessments, including the 10-Meter Walk Test (10MWT), the Timed-Up-and-Go Test, the Berg

Balance Scale, the Functional Gait Assessment, and the 6-Minute Walk Test. All assessments were administered by licensed physical therapists. If assessments were deemed unsafe or inappropriate by the physical therapist, they were skipped during that visit. Gait assessments were performed with currently prescribed assistive devices and orthotics, and therapist assistance was provided as necessary to maintain safety.

Data from the 10MWT collected before October 1, 2023 were utilized in this analysis. Similar to our previous IMU-based validation study [16], participants completed up to six trials of the 10MWT at two different speeds: comfortable velocity (CV), followed by fast velocity (FV).

Experimental setup

Equipment for this study comprised: (1) IMUs, either from Bionic Pro (Motesque, Germany) or SageMotion (SageMotion, USA), and (2) an instrumented mat – GAITRite (GAITRite Inc, USA). SageMotion was implemented in the study after Bionic Pro was commercially discontinued. Both types of IMU devices included triaxial accelerometers, gyroscopes, and magnetometers, with Bionic Pro sampling at a rate of 500 Hz and SageMotion at 100 Hz. Two IMUs were placed concurrently on the body with Velcro straps, on the left and right lower and legs (Fig. 2a). To standardize the gait analysis across all sessions and devices, we applied a rotation matrix to the SageMotion data to match the orientation of the Bionic Pro device coordinates. We used a separate system (Xsens MVN, Movella Technologies, USA), connected to the GAITRite during data collection, as a unifying system to time-synchronize recordings between sensors and the GAITRite (Fig. 2a).

A total of 116 sessions were available for analysis (80 with Bionic Pro, 36 with SageMotion). For each session, data from the IMU and GAITRite systems were visually inspected and discarded in case of the presence of significant artifacts, poor synchronization, or missing data samples. A low-pass Butterworth filter (cut-off frequency 15 Hz) was applied to the sensor data to attenuate high-frequency noise. Both the SGSA and EGSA were implemented in Matlab 2021a (Mathworks, Inc.; Natick, MA).

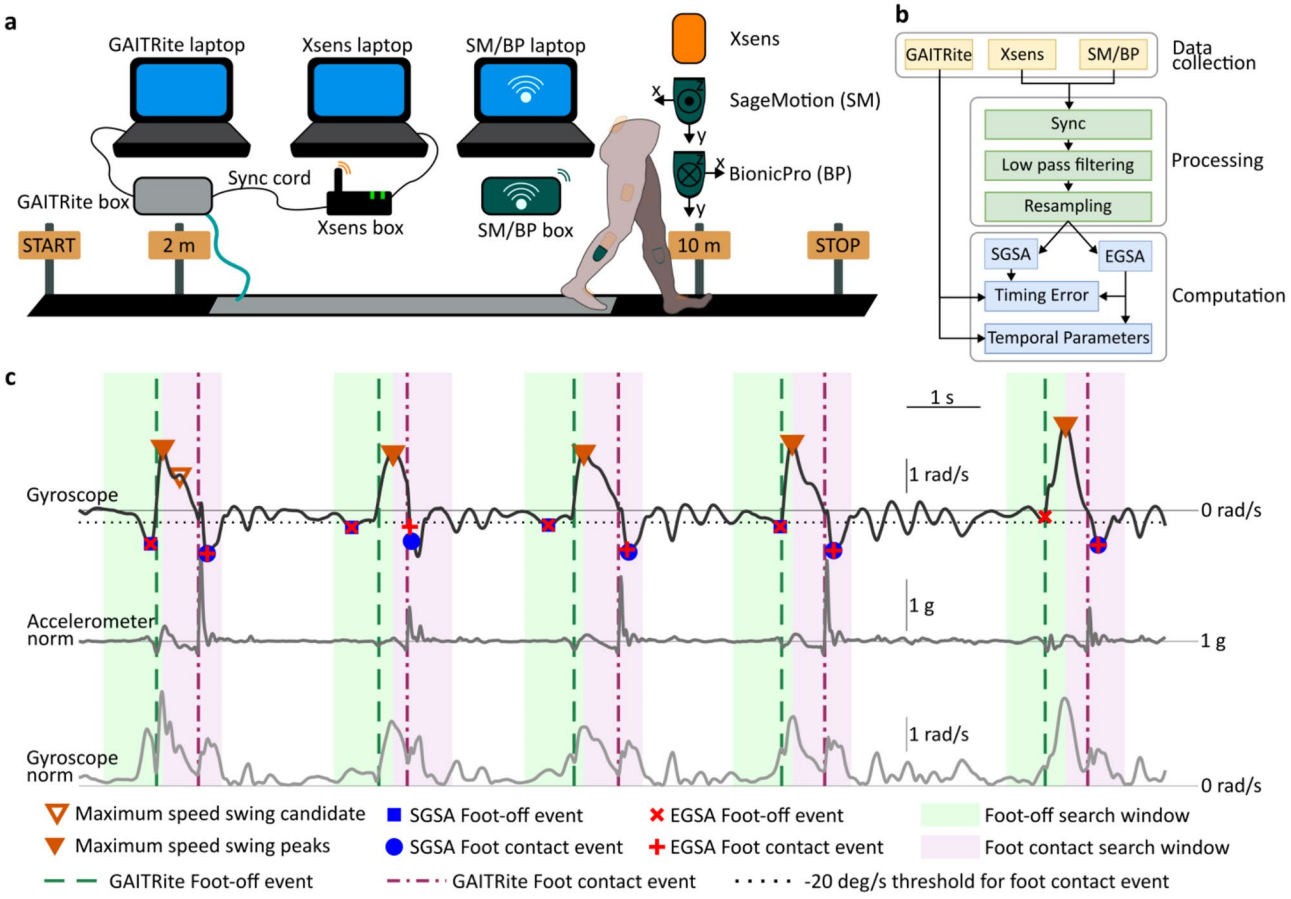

Fig. 2 Illustration of data preprocessing and the proposed algorithm. (**a**) Experimental setup for 10MWT. A system diagram for the experimental setup. Three PCs served as data recording systems for GAITRite, Xsens, and SM/BP. The laptop for SM/BP were connected to the device through WiFi. (**b**) Data processing pipeline. (**c**) Detection of FO and FC events. Sensor locations. Orange: Xsens, Green: Sensors from SM/BP were placed in mediolateral directions. Two sensors were placed adjacent to each another. Only data from the lower legs were used for this study. Data from the faded sensors was not used

Analysis 1: gait event detection

We examined the timing error (TE) of each FO and FC event, defined as the absolute difference in event timestamps between the IMU-based segmentation and the GAITRite (Eq. 1). To evaluate TE, we applied predetermined time deviation thresholds (TDTs) ranging from 0.01 to 1.0 seconds with 0.05-second increments [31], classifying the timing event T as a 'verified event' if its TE was less than or equal to the respective TDT (Eq. 2). For each threshold, we computed the cumulative percentage (CP), defined as the ratio of verified events to the total number of FO or FC gait events, N (Eq. 3).

$$TE_{ij} = \left| T_{ij_{IMU}} - T_{ij_{GAITRite}} \right| \tag{1}$$

$$VE_{ij} = \begin{cases} 1 & \text{if } \mathrm{TE_{ij}} \leq \mathrm{TDT_i} \\ 0 & \text{otherwise} \end{cases} \tag{2}$$

$$CP_j = \frac{1}{N_j} \sum_{i=1}^{N_j} VE_i \tag{3}$$

Here, *i* represents a TDT, *j* represents targeted gait events (FO or FC), and VE represents verified events. At lower TDT values, the CP reflects events with minimal timing errors, while higher thresholds include events with greater timing discrepancies.

Next, we examined CPs across different subgroups of participants based on their walking speed, gait asymmetry, and paresis, all of which can affect the gait kinematics and thus the IMU signal quality. For walking speed, participants were categorized into three subgroups based on footfall speed from the GAITRite: Slow, Medium, and Fast. We set the cutoff for these subgroups at clinically meaningful thresholds: 0.4 m/s for separating S and M, and 0.8 m/s for separating M and F, respectively, based on a commonly-used indicator of self-selected walking speed to distinguish household ambulators from community ambulators after stroke [32]. Similarly, for gait asymmetry, each step length was categorized into two subgroups using a step length symmetry index (SI), either Symmetric or Asymmetric:

$$\mathrm{SI} = \frac{|\mathrm{X_C} - \mathrm{X_P}|}{0.5 \cdot (\mathrm{X_C} + \mathrm{X_P})} \tag{4}$$

where X_C and X_P are the step lengths of the current and the previous footfalls from the GAITRite, respectively. Symmetric footfalls were then selected from individual gait cycles with SI < 0.10, which is a typical range to accommodate step-to-step symmetry variability in healthy individuals [33–35]. Asymmetric footfalls were selected from gait cycles with SI ≥ 0.10, indicating underlying unilateral impairments or, in the case of healthy individuals, occasional gait adjustments or dominant side differences. Lastly, for paresis, individual footfalls were categorized into two subgroups based on whether they experienced an affected side after stroke: Paretic or Non-Paretic. Our primary objective was to accurately compare the timing of specific gait events (FO and FC) detected by EGSA and SGSA. To achieve this, we employed TEs and CPs, which directly assess the precision and reliability of event timing relative to GAITRite's ground truth.

To compare timing errors between the EGSA and the SGSA, we categorized gait events into three groups: those where both algorithms detected the event with the identical timing (matching events), those where neither algorithm detected the event, and those where either only one algorithm detected the event or their timing did not match (not-matching events). We computed the percentage and the number of events detected by either algorithm, relative to number of events detected by the GAITRite. To compare the timing errors between the EGSA and SGSA for both FO and FC events across all subgroups, we computed the median and interquartile range (IQR) of the timing errors. Subsequently, we conducted one-tailed Mann-Whitney U test for each event type within each subgroup, resulting in 14 comparisons (2 event types in 7 subgroups). The significance level was adjusted using Bonferroni correction to $\alpha = 0.05/14 = 0.0036$ to account for multiple testing. All statistical analyses were conducted using Matlab 2021a (Mathworks, Inc.; Natick, MA).

Analysis 2: Temporal gait parameters

We computed six temporal gait parameters for each footfall using the IMU-derived gait events, including: (i) stride time (time between two consecutive FC events from the same leg), (ii) step time (time between two consecutive FC events from different legs), (iii) stance time (time between the FC and FO events from the same leg), (iv) swing time (time interval the FO and the consecutive FC from the same leg), (v) single support time (duration of the contralateral swing), and (vi) double support time (difference between stance time and single support time). These parameters were aggregated across all footfalls and trials for each participant and then compared against that participant's ground truth parameters obtained from the GAITRite. The IMU-derived temporal gait parameters were evaluated in terms of (i) reliability (using the intraclass correlation coefficient, ICC), (ii) agreement (via Bland-Altman plots), and accuracy (computed as median absolute percentage error) across (iii) walking speeds, (iv) asymmetry levels, and (v) paretic legs. This analysis is replicated from our previous work [16]. We opted not to include the SGSA in this comparative evaluation since we expected that gait events detected by the EGSA would frequently match with events detected by the SGSA in

Analysis 1, and that the EGSA would detect more events than the SGSA, resulting in a more comprehensive analysis of the EGSA with fewer undetected steps.

Results

Details about the amount of data collected and analyzed are provided in the Supplementary Material (Supplementary Fig. 1).

Analysis 1: gait event detection

Generally, the EGSA had a CP value 6% and 3% greater than the SGSA for FO (Fig. 3a) and FC (Fig. 3b), respectively, indicating that the EGSA correctly detected more gait events. At Slow walking speeds, the EGSA was more sensitive than SGSA in detecting both FO and FC events, with a respective 20% and 11% increase in detection rates. The two algorithms had similar CP values in Medium and Fast subgroups. For Asymmetric gait, the EGSA had CP values 10% and 6% greater than SGSA for the FO and FC, respectively, while performance in the Symmetric subgroup was almost equivalent. For Paretic gait and Non-Paretic gait, the EGSA slightly outperformed the SGSA in detecting the FO events for both Paretic gait (5% and 3% greater than SGSA for the FO and FC, respectively; Fig. 3a), and Non-Paretic gait (6% and 2% greater than SGSA for the FO and FC, respectively; Fig. 3b).

A significant difference in the timing error was observed between the EGSA and the SGSA for FO events

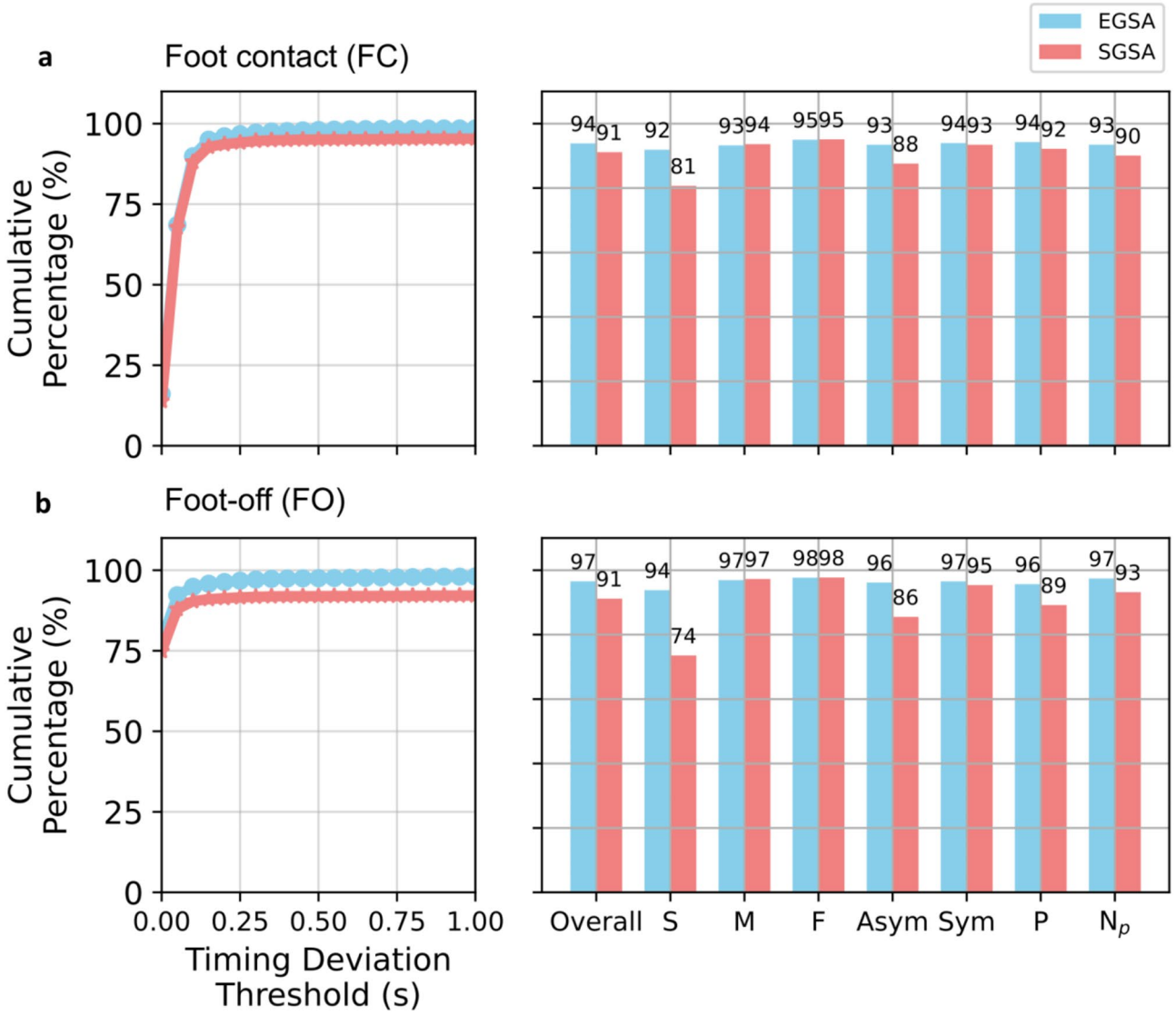

Fig. 3 Gait event detection compared between the enhanced gait segmentation algorithm (EGSA) and the Salarian gait segmentation Algorithm (SGSA). The cumulative percentage for detections of foot contact events (**a**) and foot-off events (**b**) evaluated by EGSA and SGSA. The left panels show a CP from overall data, and the right panels breakdown the CPs for subgroups. Abbreviations: S = Slow (≤ 0.4 m/s), M = Medium (0.4–0.8 m/s), F = Fast (> 0.8 m/s), Asym = Asymmetric, Sym = Symmetric, P = the paretic leg, N_p = the non-paretic leg

in both the Slow and Asymmetric subgroups (p's<0.001). No significant differences were found in the other subgroups. Most gait events were detected by both the EGSA and SGSA, suggesting a strong baseline performance in standard gait scenarios.

A detailed timing error analysis for gait event detection by the EGSA and SGSA is presented across subgroups in Table 2. For FC events, the EGSA demonstrated lower timing errors than the SGSA for the Paretic subgroup of footfalls ($p<0.01$). For FO events, the EGSA demonstrated lower timing errors than the SGSA for the Slow, Asymmetric, and Non-Paretic subgroups (p's<0.001). Similarly, for FO events, the EGSA demonstrated lower median and IQR compared to the SGSA in the Slow, Asymmetric, and Non-Paretic subgroups.

Analysis 2: temporal gait parameters

Numerical results are detailed in Table 3. Stride time, step time, stance time, and double support time estimates all achieved an excellent level of reliability (ICC>0.90). Swing time and single support time estimates had poor reliability (ICC<0.50). Only a small fraction of footfalls (ranging between 1.84 and 4.04%) fell outside the limits of agreement (LoA), ranging from 0.36 to 0.70 s for all estimates.

Stride time was estimated without any systematic or proportional bias in the error (Fig. 4a). Median absolute percentage error (MdAPE, Fig. 4b) significantly decreased in both the medium (-0.97%, $p<0.001$) and fast (-1.26%, $p<0.001$) speed subgroups compared to the slow speed subgroup, and for symmetric compared to asymmetric footfalls (-0.52%, $p<0.001$). MdAPE of the stride time estimate significantly differed between paretic (1.59%) and non-paretic leg (1.15%).

The step time estimate (Fig. 4c) was significantly proportionally underestimated following an intercept of 0.01s ($p=0.02$) and slope of -0.01 ($p=0.01$). MdAPE was significantly lower in the medium (-1.37%, $p<0.001$) and fast (-2.72%, $p<0.001$) speed subgroups compared to the slow subgroup, in the symmetric with respect to the asymmetric subgroups (-2.44%, $p<0.001$), and in the paretic leg compared to the non-paretic one (-0.67%, $p<0.001$) (Fig. 4d).

A significant constant bias of -0.07s ($p<0.001$) was found for the stance time estimate (Fig. 4e). MdAPE was significantly lower in the slow speed subgroup compared to both the medium (-3.83%, $p<0.001$) and fast (-3.30%, $p<0.001$) speed subgroups. We also find a significant decrease in the MdAPE by 1.63% ($p<0.001$) for asymmetric footfalls compared to symmetric footfalls, and by 0.34% ($p<0.001$) for non-paretic footfalls compared to the paretic ones (Fig. 4f).

Swing time was estimated with a significant proportional bias (intercept 0.42s, slope -0.78, $p<0.001$, Fig. 4g). MdAPE was significantly different across subgroups, achieving optimal performance in the fast speed, symmetric, and paretic side subgroups (Fig. 4h).

Single support time, computed as the time of the contralateral swing, achieved almost equal performance with the swing time estimate (Fig. 4i-j).

Double support time was significantly underestimated (Fig. 4k), following a proportional bias (intercept -0.14s, slope -0.02, $p<0.001$). MdAPE was significantly lower in the slow speed and asymmetric subgroups, whereas no change was identified between sides (Fig. 4l).

Discussion

This study introduced and characterized the EGSA, a population-specific method for gait event detection, using two lower leg IMUs for individuals with stroke in IRFs. Unlike the original SGSA, which was designed and validated for Parkinson's disease patients using solely gyroscopic data, the EGSA incorporates both accelerometer and gyroscope inputs to accommodate the asymmetrical and variable gait patterns of stroke survivors. Hemiparesis often results in uneven stride lengths, altered stance and swing durations, and inconsistent shank movements, which can confound traditional segmentation methods that rely on uniform gait cycles.

Overall, the EGSA improved detection of FO and FC compared to the SGSA. This enhancement was particularly evident in the timely detection of FO for individuals with slower and asymmetric gait patterns. Temporal gait parameters from the EGSA achieved lower percentage absolute error at medium-to-fast gait speed, and in the symmetric subgroup. FO detection benefited the most from the EGSA, with the cumulative percentage of FO detection increasing up to 11% and 15% within the Slow and Asymmetric subgroups, respectively. This increase translated fewer timing errors, signifying more precisely timed detections (Table 2).

In contrast to previous studies employing fixed time thresholds for detection rate evaluation (such as 300 ms [36] or 500 ms [37]), our assessment method provided a comprehensive view of the EGSA's performance in detecting gait events. This approach is particularly crucial as it offers a more detailed understanding of algorithm behavior across diverse clinical scenarios. The SGSA exhibited satisfactory performance in less impaired populations, but demonstrated limitations in addressing the complexities presented by individuals with slower and asymmetric gait patterns. In such cases, the EGSA achieved more accurate gait event detections.

Temporal gait parameters from the EGSA revealed varied performance across different subgroups. We expect that the reduced reliability of swing and single support phase estimates is due to the larger impact of detection errors on these shorter metrics compared to stride, step,

Table 2 Timing error analysis for gait event segmentation by the EGSA and the SGSA across subgroups. Each entry includes the percentage of event counts detected by either the EGSA or the SGSA, relative to event detections by the GR, and the number of detected events, indicated within brackets. The penultimate and antepenultimate columns from the far right column of the table show the median and IQR of timing errors for the EGSA and the SGSA, respectively. The far-right column of the table provides results from a statistical test, specifically comparing the timing accuracy of detections between the two methods. Abbreviations: S = slow (≤ 0.4 m/s), M = medium (0.4–0.8 m/s), F = fast (> 0.8 m/s), Asym = asymmetric, Sym = symmetric, P = the paretic leg, $\boldsymbol{N_p}$ = the non-paretic leg

Event Type	Sub Group	Number of events detected by GAITRite	Number of matching events detected by both EGSA & SGSA	Number of events undetected by both SGSA & EGSA	Number of not-matching events detected by both EGSA and SGSA	Number of not-matching events detected by EGSA	Number of not-matching events detected by SGSA	Median [IQR] of TEs by EGSA	Median [IQR] of TEs by SGSA	Statistical significance in Timing Error (Mann-Whitney U test *p*-value)
FO	S	1221	74.77% (913)	0.74% (9)	24.49% (299)	99.00% (296)	7.02% (21)	0.00 [0.28]	3.32 [4.64]	**< 6.63 x** 10^{-10}
	M	837	98.09% (821)	1.55% (13)	0.36% (3)	0.00% (0)	100.00% (3)	-	-	-
	F	1972	98.17% (1936)	1.72% (34)	0.10% (2)	50.00% (1)	100.00% (2)	-	-	-
	Asym	2069	86.61% (1792)	0.68% (14)	12.71% (263)	99.62% (262)	6.08% (16)	0.00 [0.24]	3.60 [2.41]	**< 2.92 x** 10^{-9}
	Sym	1962	95.77% (1879)	2.14% (42)	2.09% (41)	85.37% (35)	24.39% (10)	0.05 [0.35]	0.02 [14.17]	0.15
	P	2498	90.99% (2273)	1.24% (31)	7.77% (194)	97.94% (190)	7.73% (15)	0.00 [0.43]	0.02 [4.56]	0.21
	N_p	2471	93.16% (2302)	1.01% (25)	5.83% (144)	97.92% (141)	16.67% (24)	0.00 [0.10]	3.43 [4.46]	**< 3.42 x** 10^{-6}
FC	S	1221	63.31% (773)	0.66% (8)	36.04% (440)	99.09% (436)	67.73% (298)	0.04 [0.11]	0.04 [0.07]	0.03
	M	837	70.13% (587)	1.55% (13)	28.32% (237)	98.73% (234)	100.00% (237)	0.02 [0.04]	0.02 [0.03]	0.35
	F	1972	74.85% (1476)	1.72% (34)	23.43% (462)	99.78% (461)	100.00% (462)	0.02 [0.03]	0.02 [0.02]	0.31
	Asym	2069	69.02% (1428)	0.68% (14)	30.30% (627)	99.84% (626)	79.90% (501)	0.04 [0.10]	0.04 [0.07]	0.12
	Sym	1962	71.81% (1409)	2.09% (41)	26.10% (512)	98.63% (505)	96.88% (496)	0.02 [0.04]	0.02 [0.03]	0.10
	P	2498	72.06% (1800)	1.20% (30)	26.74% (668)	99.25% (663)	93.41% (624)	0.02 [0.07]	0.02 [0.05]	< 0.01
	N_p	2471	70.34% (1738)	1.01% (25)	28.65% (708)	99.58% (705)	86.16% (610)	0.03 [0.06]	0.03 [0.05]	0.63

Table 3 Temporal gait parameters (median and interquartile range) from each system, as well as reliability (ICC), agreement (b ± LoA), and accuracy (MdAPE) of the EGSA relative to the GR across subgroups. N is the number of instances for each temporal parameter

Parameter	ICC	b ± LoA (s)	MdAPE Ov (%)	MdAPE Subgroup (%)		*p* value
Stride time ($n = 3958$)	0.979	-0.003 ± 0.397	1.33 [2.64]	S	2.31 [5.40]	< 0.001 (S vs. M)
				M	1.34 [2.38]	< 0.001 (S vs. F)
				F	1.05 [1.76]	< 0.001 (M vs. F)
				Sym	1.12 [1.94]	< 0.001
				Asym	1.64 [3.34]	
				P	1.59 [3.01]	< 0.001
				N_p	1.15 [2.19]	
Step time ($n = 4418$)	0.953	0.001 ± 0.360	3.66 [6.31]	S	5.46 [7.67]	< 0.001 (S vs. M)
				M	4.09 [6.78]	< 0.001 (S vs. F)
				F	2.74 [4.77]	< 0.001 (M vs. F)
				Sym	2.61 [4.46]	< 0.001
				Asym	5.05 [7.81]	
				P	3.33 [5.51]	< 0.001
				N_p	4.00 [7.38]	
Stance time ($n = 3985$)	0.958	-0.076 ± 0.524	8.56 [7.98]	S	6.14 [8.32]	< 0.001 (S vs. M)
				M	9.97 [7.33]	< 0.001 (S vs. F)
				F	9.44 [7.01]	0.999 (M vs. F)
				Sym	9.33 [6.48]	< 0.001
				Asym	7.70 [9.02]	
				P	8.84 [8.62]	< 0.001
				N_p	8.50 [7.22]	
Swing time ($n = 3958$)	0.410	0.069 ± 0.453	21.49 [23.18]	S	34.00 [44.32]	< 0.001 (S vs. M)
				M	23.72 [21.91]	< 0.001 (S vs. F)
				F	17.33 [15.32]	< 0.001 (M vs. F)
				Sym	18.48 [15.61]	< 0.001
				Asym	25.49 [33.57]	
				P	19.91 [21.96]	< 0.001
				N_p	23.24 [24.45]	
Single support time ($n = 3958$)	0.410	0.069 ± 0.453	22.13 [24.30]	S	35.19 [44.94]	< 0.001 (S vs. M)
				M	24.00 [21.94]	< 0.001 (S vs. F)
				F	17.32 [15.43]	< 0.001 (M vs. F)
				Sym	18.63 [16.44]	< 0.001
				Asym	26.20 [33.57]	
				P	23.24 [24.45]	< 0.001
				N_p	19.91 [21.96]	
Double support time ($n = 3954$)	0.901	-0.158 ± 0.704	31.12 [27.04]	S	17.62 [19.75]	< 0.001 (S vs. M)
				M	29.92 [20.09]	< 0.001 (S vs. F)
				F	40.34 [22.87]	< 0.001 (M vs. F)
				Sym	36.21 [22.01]	< 0.001
				Asym	25.63 [27.41]	
				P	31.54 [27.18]	0.855
				N_p	31.53 [26.62]	

and stance time estimates, leading to greater variability and potentially decreased ICC values. Results aligned with our previous finding [16], yet they used different sensor systems and algorithm for foot motion monitoring. Importantly, the observed biases were generally more pronounced than in the previous study, potentially attributed to the range of impairments encompassed in our population. This diversity, reflected in a walking speed range of 0.03 to 2.00 m/s, slower than the 0.24 to 2.40 m/s range of our previous study, emphasizes the real-world applicability of our findings to a more extensive spectrum of stroke-related gait abnormalities. Additional methodological differences could account for the systematic biases between the EGSA and GAITRite. For instance, whereas the GAITRite measures plantar pressure directly beneath the foot, the EGSA's sensors are located on the shank. This spatial difference means that shank movements may not perfectly synchronize with

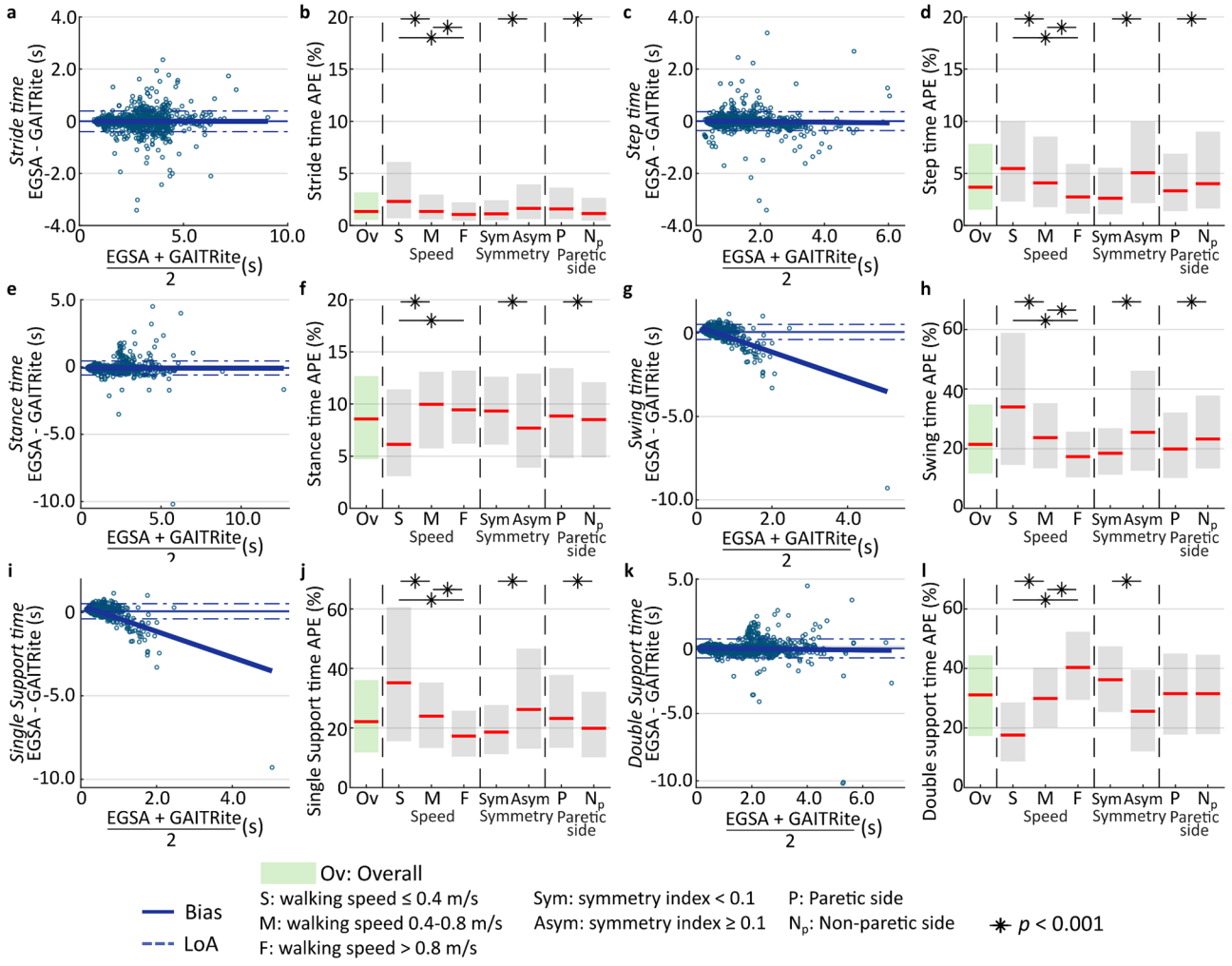

Fig. 4 Temporal gait parameter estimates of the EGSA compared to GAITRite. Bland–Altman plot, and speed-/asymmetry-/paretic side- error analyses for (**a**)–(**b**) stride time, (**c**)-(**d**) step time, (**e**)–(**f**) stance time, (**g**)–(**h**) swing time, (**i**)-(**j**) stride support time, (**k**)–(**l**) double support time. Boxes range from the 25th to the 75th percentiles and the intermediate line represents the median value. Significant difference between error across speed ranges and asymmetry levels in (**b**), (**d**), (**f**), (**h**), (**j**) and (**l**) was indicated an asterisk (*, $p < 0.001$)

foot contact events. Thus, future work should also consider validating the EGSA against other gold standard, high-resolution systems, such as optical motion capture, so that potential differences from sensor positioning can be quantified.

Our hypothesis regarding larger errors for slow and asymmetric subgroups was supported, with some exceptions noted for the stance and double support estimates. These exceptions, particularly the significantly lower MdAPE at slow walking speeds compared to medium and fast speeds, can be attributed to the use of the MdAPE. The discrepancy arises due to the absolute error being small when contrasted with the reference value that is very large at slow speeds. Furthermore, the breakdown of error between sides highlighted increased errors in step time and swing phase estimates on the non-paretic side, as reflected by the difference in timing accuracy between the paretic and non-paretic sides (Table 2). This aligns with biomechanical expectations, as weight transfers forward, while the paretic leg bears the weight. Due to weakness or impaired motor control on the paretic leg, stroke survivors often rely more heavily on their non-paretic leg to maintain stability and generate propulsive forces in gait, making the swing of the non-paretic leg quick. The SGSA may struggle to accurately identify these compensatory FO events.

Gait event segmentation algorithms hold promise when applied during clinical assessments or ongoing treatments. These algorithms segment gait sequences into individual strides, offering valuable insights into an individual's gait dynamics. Various measurement systems have been proposed for this purpose, including plantar pressure measurement [38], optical motion capture systems [39], camera-based computer vision systems [40],

and IMUs [23, 41]. Among these, IMUs are not confined by spatial limitations such as occlusions and can track movements in naturalistic settings, allowing clinicians to administer therapy without the constraints of fixed equipment. Several gait analysis systems based on IMU have been developed, each with varying sensor placement on the body (such as the foot, pelvis, and legs) and segmentation algorithms, resulting in different levels of performance. However, the strict regulation and close monitoring of therapy dosage in IRFs can sometimes hinder the integration of technology. Limitations in time, perceived lack of benefits, and reimbursement challenges may lead to reduced implementation [42]. Hence, more validation studies are necessary to support the optimal adoption of this technology, facilitating a quick and informed utilization.

The EGSA, with its robust application to slow and asymmetric walkers, presents a practical solution for IRFs, automating the measurement of temporal gait parameters with minimal requirement of sensors on a patient body. Our ultimate goal is to adapt the EGSA to clinical care; by accurately detecting gait events in real-time, the EGSA enables clinicians to make more informed decisions about therapy adjustments in real-time. Unlike approaches requiring cumbersome laboratory equipment, the EGSA offers a balance of accuracy and practicality for clinicians working in the IRF setting and beyond. This positions EGSA as a more adaptable tool compared to the existing methodologies employing computer vision, aligning with studies that emphasize the need for efficient and accurate gait analysis in clinical settings.

This study has several limitations. The biomechanically driven enhancements in the algorithm were based on the assumption that fundamental gait events are visible in the sensor signals of the lower legs. The availability of a comprehensive annotated dataset played a crucial role in refining these conditions, yet ongoing efforts can further enhance the algorithm's detection rate. Similarly, the template for DTW FC detection was constructed from signals of healthy controls, therefore neglecting the post-stroke gait diversity. However, because the array of impairments present in individuals after a stroke is wide-ranging, the definition of a unique template valid for the full spectrum of impairments is challenging. Analysis-wise, the imbalance in data incorporation across different time points may affect the analysis. Secondly, the limited data samples in each subgroup led to reduced statistical power in the Mann-Whitney U test. Lastly, the absence of some participants post-hospital discharge resulted in fewer events recorded at later time points post-stroke; however, we believe this does not significantly impact the validity of our analysis because we showed an equivalent performance between SGSA and EGSA when applied to the chronic phase of the stroke.

These methods can be utilized with other conventional IMUs as well, as demonstrated by our ability to implement them in two different brands of sensors. Although it may add complexity to the setup, adding sensors on the feet and information from other modalities (i.e., magnetometer) may further enhance performance and facilitate the computation of spatial parameters [43]. Our proposed approach aims to reduce complexity of the sensor system by utilizing only lower leg IMUs, thereby simplifying implementation in patient care units. Overall, we expect the EGSA to be a more robust approach to IMU-based gait segmentation across healthy and clinical populations with different gait impairments. While we have demonstrated that the EGSA offers population-specific improvements for post-stroke gait segmentation, future work will investigate its applicability as a generic, trans-diagnostic gait segmentation tool by testing its performance across various clinical populations.

Conclusions

The study developed and validated an enhanced gait segmentation algorithm for inertial sensors, demonstrating its efficacy in detecting gait events among patients undergoing post-stroke rehabilitation. This advancement addresses the limitations of existing gait analysis methods, especially in clinical populations with a broad range of impairments. This enhancement offers a contribution to rehabilitation medicine by providing clinicians with a reliable, non-invasive method for detailed gait analysis using two leg-worn sensors. Future applications of this algorithm can facilitate personalized rehabilitation planning, monitor progress, and ultimately contribute to better patient outcomes in inpatient rehabilitation facilities.

Abbreviations

10MWT	10-Meter Walk Test
APE	Absolute percentage error
Asym	Asymmetric
BP	Bionic Pro
CP	Cumulative percentage
CV	Comfortable velocity
DTW	Dynamic time warping
EGSA	Enhanced gait segmentation algorithm
F	Fast
FC	Foot contact
FO	Foot-off
FV	Fast velocity
GR	GAITRite
ICC	Intra-class correlation coefficient
IMU	Inertial measurement unit
IRF	Inpatient Rehabilitation Facility
M	Medium
MdAPE	Median absolute percentage error
S	Slow
SGSA	Salarian gait segmentation algorithm
SI	Symmetry index
SM	SageMotion
Sym	Symmetric

TDT Time deviation threshold
TE Timing error

Supplementary Information

The online version contains supplementary material available at https://doi.org/10.1186/s12984-024-01521-8.

Supplementary Material 1

Supplementary Material 2

Acknowledgements
The authors would like to thank Shreya Aalla, Joe Harris, Kristine Buchler, Jennifer Traines, Kelly McKenzie, Matt McGuire, Kate Enzler, Caitlin Deom, and Sara Prokup for their contribution to recruitment and data collection.

Author contributions
Conceptualization: AJ, MO. Methodology: All authors. Software: FL. Validation: FL, SO. Formal analysis: FL, SO. Investigation: FL, SO, MO. Resources: AJ. Data Curation: FL, SO. Writing – original draft preparation: FL, SO. Writing – review and editing: All authors. Visualization: FL, SO. Supervision: MO. Project administration: AJ. Funding acquisition: AJ.

Funding
This work was supported by the National Institute on Disability, Independent Living, and Rehabilitation Research (90REGE0010).

Data availability
No datasets were generated or analysed during the current study.

Declarations

Ethics approval and consent to participate
The study was approved by the Institutional Review Board of Northwestern University (Chicago, IL; STU00205532) under federal regulations, university policies, and ethical standards regarding research on human subjects.

Consent for publication
Not applicable.

Competing interests
The authors declare no competing interests.

Received: 29 August 2024 / Accepted: 3 December 2024
Published online: 21 December 2024

References

1. Thewlis D, Bishop C, Daniell N, Paul G. 'A comparison of two commercially available motion capture systems for gait analysis: high-end vs low-cost', Congress of the International Society of Biomechanics, 2011, Accessed: Nov. 30, 2022. [Online]. Available: http://www.isb2011.org/welcome.html
2. Lee J, Shin SY, Ghorpade G, Akbas T, Sulzer J. 'Sensitivity comparison of inertial to optical motion capture during gait: Implications for tracking recovery', IEEE International Conference on Rehabilitation Robotics, vol. 2019-June, pp. 139–144, Jun. 2019, https://doi.org/10.1109/ICORR.2019.8779411
3. Lanotte F, O'Brien MK, Jayaraman A. 'AI in Rehabilitation Medicine: Opportunities and Challenges', Ann Rehabil Med, vol. 47, no. 6, pp. 444–458, Dec. 2023, https://doi.org/10.5535/ARM.23131
4. Celik Y, Stuart S, Woo WL, Godfrey A. Gait analysis in neurological populations: progression in the use of wearables. Med Eng Phys. Jan. 2021;87:9–29. https://doi.org/10.1016/J.MEDENGPHY.2020.11.005.
5. O'Brien MK, et al. Wearable sensors improve prediction of Post-stroke walking function following Inpatient Rehabilitation. IEEE J Transl Eng Health Med. 2022;10. https://doi.org/10.1109/JTEHM.2022.3208585.
6. O'Brien MK, et al. Early Prediction of Poststroke Rehabilitation outcomes using Wearable sensors. Phys Ther. Jan. 2024;23. https://doi.org/10.1093/PTJ/PZAD183.
7. O'Brien MK, Hohl K, Lieber RL, Jayaraman A, Shirley A, Abilitylab R. 'Automate, Illuminate, Predict: A Universal Framework for Integrating Wearable Sensors in Healthcare', Digit Biomark, vol. 8, no. 1, pp. 149–158, Jun. 2024, https://doi.org/10.1159/000540492
8. Jayashree LS, Madhana K, Preethish Kumar V, Swathi S, Soundharyan P. Jan., 'A Quantitative Gait Assessment Approach Using a Wearable Device and Its Validation for Different Neurological Disorder Conditions', Top Geriatr Rehabil, vol. 40, no. 1, pp. 19–36, 2024, https://doi.org/10.1097/TGR.0000000000000419
9. Hsu WC et al. 'Multiple-Wearable-Sensor-Based Gait Classification and Analysis in Patients with Neurological Disorders', Sensors., 2018, Vol. 18, Page 3397, vol. 18, no. 10, p. 3397, Oct. 2018, https://doi.org/10.3390/S18103397
10. Zhu S et al. 'Gait Analysis with Wearables Is a Potential Progression Marker in Parkinson's Disease', Brain Sciences., 2022, Vol. 12, Page 1213, vol. 12, no. 9, p. 1213, Sep. 2022, https://doi.org/10.3390/BRAINSCI12091213
11. Lonini L, Gupta A, Deems-Dluhy S, Hoppe-Ludwig S, Kording K, Jayaraman A. 'Activity Recognition in Individuals Walking With Assistive Devices: The Benefits of Device-Specific Models', JMIR Rehabil Assist Technol, vol. 4, no. 2, p. e8, Aug. 2017, https://doi.org/10.2196/rehab.7317
12. Muro-de-la-Herran A, García-Zapirain B, Méndez-Zorrilla A. 'Gait Analysis Methods: An Overview of Wearable and Non-Wearable Systems, Highlighting Clinical Applications', Sensors 2014, Vol. 14, Pages 3362–3394, vol. 14, no. 2, pp. 3362–3394, Feb. 2014, https://doi.org/10.3390/S140203362
13. Tao W, Liu T, Zheng R, Feng H. 'Gait Analysis Using Wearable Sensors', Sensors 2012, Vol. 12, Pages 2255–2283, vol. 12, no. 2, pp. 2255–2283, Feb. 2012, https://doi.org/10.3390/S120202255
14. Winstein CJ et al. Jun., 'Guidelines for Adult Stroke Rehabilitation and Recovery: A Guideline for Healthcare Professionals From the American Heart Association/American Stroke Association', Stroke, vol. 47, no. 6, pp. e98–e169, 2016, https://doi.org/10.1161/STR.0000000000000098
15. Wang Y, et al. Gait characteristics of post-stroke hemiparetic patients with different walking speeds. Int J Rehabil Res. Mar. 2020;43(1):69. https://doi.org/10.1097/MRR.0000000000000391.
16. Lanotte F, Shin SY, O'Brien MK, Jayaraman A. Validity and reliability of a commercial wearable sensor system for measuring spatiotemporal gait parameters in a post-stroke population: the effects of walking speed and asymmetry. Physiol Meas Aug. 2023. https://doi.org/10.1088/1361-6579/ACEECF.
17. Olney SJ, Richards C. 'Hemiparetic gait following stroke. Part I: Characteristics', Gait Posture, vol. 4, no. 2, pp. 136–148, Apr. 1996, https://doi.org/10.1016/0966-6362(96)01063-6
18. Yang S, Zhang JT, Novak AC, Brouwer B, Li Q. 'Estimation of spatio-temporal parameters for post-stroke hemiparetic gait using inertial sensors', Gait Posture, vol. 37, no. 3, pp. 354–358, Mar. 2013, https://doi.org/10.1016/J.GAITPOST.2012.07.032
19. Fukuchi CA, Fukuchi RK, Duarte M. Effects of walking speed on gait biomechanics in healthy participants: a systematic review and meta-analysis. Syst Rev. Jun. 2019;8(1):1–11. https://doi.org/10.1186/S13643-019-1063-Z/FIGURES/6.
20. Salarian A et al. Aug., 'Gait assessment in Parkinson's disease: toward an ambulatory system for long-term monitoring', IEEE Trans Biomed Eng, vol. 51, no. 8, pp. 1434–1443, 2004, https://doi.org/10.1109/TBME.2004.827933
21. Ebersbach G et al. Jul., 'Comparative analysis of gait in Parkinson's disease, cerebellar ataxia and subcortical arteriosclerotic encephalopathy', Brain, vol. 122, no. 7, pp. 1349–1355, 1999, https://doi.org/10.1093/BRAIN/122.7.1349
22. Trojaniello D et al. Nov., 'Estimation of step-by-step spatio-temporal parameters of normal and impaired gait using shank-mounted magneto-inertial sensors: Application to elderly, hemiparetic, parkinsonian and choreic gait', J Neuroeng Rehabil, vol. 11, no. 1, pp. 1–12, 2014, https://doi.org/10.1186/1743-0003-11-152/FIGURES/4
23. Mao Y, Ogata T, Ora H, Tanaka N, Miyake Y. 'Estimation of stride-by-stride spatial gait parameters using inertial measurement unit attached to the shank with inverted pendulum model', Scientific Reports 2021 11:1, vol. 11, no. 1, pp. 1–10, Jan. 2021, https://doi.org/10.1038/s41598-021-81009-w
24. Liuzzi P, et al. Machine learning based estimation of dynamic balance and gait adaptability in persons with neurological diseases using inertial sensors. Sci Rep 2023. May 2023;13(1):1. https://doi.org/10.1038/s41598-023-35744-x.
25. Li S, Francisco GE, Zhou P. Post-stroke hemiplegic gait: New perspective and insights', Front Physiol. No AUG. Aug. 2018;9. https://doi.org/10.3389/FPHYS.2018.01021/BIBTEX.

26. Sackley CM. Falls, sway, and symmetry of weight-bearing after stroke. Int Disabil Stud. 1991;13(1):1–4. https://doi.org/10.3109/03790799109166267.
27. Casey Kerrigan D, Mark Karvosky ME, Patrick Riley MO, Kerrigan C, Kinetics J. 'Spastic Paretic Stiff-Legged Gait', 2001. [Online]. Available: http://journals.lww.com/ajpmr
28. Kim CM, Eng JJ. Magnitude and pattern of 3D kinematic and kinetic gait profiles in persons with stroke: relationship to walking speed. Gait Posture. Oct. 2004;20(2):140–6. https://doi.org/10.1016/J.GAITPOST.2003.07.002.
29. Beyaert C, Vasa R, Frykberg GE. 'Gait post-stroke: Pathophysiology and rehabilitation strategies', Neurophysiologie Clinique/Clinical Neurophysiology, vol. 45, no. 4–5, pp. 335–355, Nov. 2015, https://doi.org/10.1016/J.NEUCLI.2015.09.005
30. Aminian K, Najafi B, Ula CB, Leyvraz P-F, Robert P. Spatio-temporal parameters of gait measured by an ambulatory system using miniature gyroscopes. J Biomech. 2002;35:689–99.
31. French MA, Koller C, Arch ES. Comparison of three kinematic gait event detection methods during overground and treadmill walking for individuals post stroke. J Biomech. Jan. 2020;99:109481. https://doi.org/10.1016/J.JBIOMECH.2019.109481.
32. Perry J, Garrett M, Gronley JAK, Mulroy SJ. 'Classification of Walking Handicap in the Stroke Population', Stroke, vol. 26, no. 6, pp. 982–989, 1995, https://doi.org/10.1161/01.STR.26.6.982
33. Kodesh E, Kafri M, Dar G, Dickstein R. Walking speed, unilateral leg loading, and step symmetry in young adults. Gait Posture. Jan. 2012;35(1):66–9. https://doi.org/10.1016/J.GAITPOST.2011.08.008.
34. Patterson KK, Nadkarni NK, Black SE, McIlroy WE. Gait symmetry and velocity differ in their relationship to age. Gait Posture. Apr. 2012;35(4):590–4. https://doi.org/10.1016/J.GAITPOST.2011.11.030.
35. Zadik S, Benady A, Gutwillig S, Florentine MM, Solymani RE, Plotnik M. 'Age related changes in gait variability, asymmetry, and bilateral coordination – When does deterioration starts?', Gait Posture, vol. 96, pp. 87–92, Jul. 2022, https://doi.org/10.1016/J.GAITPOST.2022.05.009
36. Pham MH et al. Sep., 'Validation of a step detection algorithm during straight walking and turning in Patients with Parkinson's disease and older adults using an inertial measurement unit at the lower back', Front Neurol, vol. 8, no. SEP, p. 281095, 2017, https://doi.org/10.3389/FNEUR.2017.00457/BIBTEX
37. Micó-Amigo ME, et al. Assessing real-world gait with digital technology? Validation, insights and recommendations from the Mobilise-D consortium. J Neuroeng Rehabil. Dec. 2023;20(1):1–26. https://doi.org/10.1186/S12984-023-01198-5/TABLES/6.
38. Martini E et al. Mar., 'Pressure-Sensitive Insoles for Real-Time Gait-Related Applications', Sensors, vol. 20, no. 5, p. 1448, 2020, https://doi.org/10.3390/s20051448
39. Wang L, Li Y, Xiong F, Zhang W. 'Gait Recognition Using Optical Motion Capture: A Decision Fusion Based Method', Sensors 2021, Vol. 21, Page 3496, vol. 21, no. 10, p. 3496, May 2021, https://doi.org/10.3390/S21103496
40. Tang Y, Li Z, Tian H, Ding J, Lin B. 'Detecting Toe-Off Events Utilizing a Vision-Based Method', Entropy 2019, Vol. 21, Page 329, vol. 21, no. 4, p. 329, Mar. 2019, https://doi.org/10.3390/E21040329
41. Prasanth H et al. 'Wearable Sensor-Based Real-Time Gait Detection: A Systematic Review', Sensors., 2021, Vol. 21, Page 2727, vol. 21, no. 8, p. 2727, Apr. 2021, https://doi.org/10.3390/S21082727
42. Chen CC, Bode RK. Factors influencing therapists' decision-making in the acceptance of new technology devices in stroke rehabilitation. Am J Phys Med Rehabil. May 2011;90(5):415–25. https://doi.org/10.1097/PHM.0B013E318214F5D8.
43. Arens P, et al. Real-time gait metric estimation for everyday gait training with wearable devices in people poststroke. Wearable Technol. 2021;2:e2. https://doi.org/10.1017/WTC.2020.11.

Publisher's note